ELSEVIER

Journal of Structural Geology 26 (2004) 967–982

JOURNAL OF STRUCTURAL GEOLOGY

www.elsevier.com/locate/jsg

Coevolution of crack-seal texture and fracture porosity in sedimentary rocks: cathodoluminescence observations of regional fractures

S.E. Laubach[a,*], R.M. Reed[a], J.E. Olson[b], R.H. Lander[a,c], L.M. Bonnell[a,c]

[a]*Bureau of Economic Geology, John A. and Katherine G. Jackson School of Geosciences, The University of Texas at Austin, Austin, TX 78713, USA*
[b]*Department of Petroleum and Geosystems Engineering, The University of Texas at Austin, Austin, TX 78713, USA*
[c]*Geocosm L.L.C., 3311 San Mateo Drive, Austin, TX 78738, USA*

Received 2 May 2002; accepted 16 August 2003

Abstract

This paper examines evidence of coupled diagenetic and mechanical processes within growing fractures in sandstones: crack-seal texture and associated, concurrently produced fracture porosity. Crack-seal textures in narrow mineral bridges associated with fracture porosity are common in regional fractures formed at moderate to great depth (>1000– ~ 6000 m) in quartz-cemented sandstones that otherwise lack significant structure. Use of SEM-based cathodoluminescence systems and superposition of images collected using color filters accurately delineate crack-seal increments in fracture-bridging quartz cement. Bridges and crack-seal texture mark competition between cement precipitation and opening rates during opening-mode fracture growth. These structures document episodic fracture growth that can include tens to hundreds of widening increments in fractures having apertures of a few tens of microns to several millimeters or more. These structures are not the product of unique circumstances in burial history and fluid flow but, rather, reflect the confluence of rock-dominated geochemistry that is widespread in time and space and fracturing caused by a spectrum of loading conditions.

Keywords: Fracture porosity; Diagenesis; Crack-seal texture; Fluid flow; Quartz cement

1. Introduction

Essential to progress in the understanding of fracture patterns is appreciation of chemical processes in growth of opening-mode fracture systems. For fractures in sedimentary rocks in diagenetic environments (>1000– ~ 6000 m depth), where fractures are new rock surfaces created in the presence of high temperatures and reactive fluids, effects of mineral precipitation and dissolution (diagenesis) on fracture attributes and growth could be significant. Observations of core samples show that fractures from these settings typically contain at least some authigenic cement. Yet dynamic evolution of coupled diagenetic reactions and fracture mechanics and their effects on fracture attributes remain largely unknown. We illustrate the importance of interacting mechanical and diagenetic processes in sandstones during fracture growth by describing a widespread but little-appreciated by-product of these linked processes, namely crack-seal texture and associated fracture porosity.

Crack-seal texture is the result of repeated fracturing during cement precipitation within fractures (Figs. 1 and 2). Thus, it is emblematic of coupled mechanical and diagenetic interaction. Although previously documented primarily in veins in low-temperature metamorphic rocks and faults (Ramsay, 1980; Anders and Wiltschko, 1994), crack-seal texture is also a common, but little appreciated, attribute of opening-mode fractures in slightly deformed and nearly flat lying sedimentary rocks. Moreover, as discussed later, owing to advances in microscopy, fine-scale observations are now possible that provide insight into the origin and development of these structures.

2. Sample suite

Our conclusions are based on documentation of definitive crack-seal textures in 24 sandstone units and observations of weakly developed or somewhat ambiguous

* Corresponding author. Tel.: +1-512-471-6303; fax: +1-512-471-0140.
E-mail address: steve.laubach@beg.utexas.edu (S.E. Laubach).

0191-8141/$ - see front matter © 2004 Elsevier Ltd. All rights reserved.
doi:10.1016/j.jsg.2003.08.019

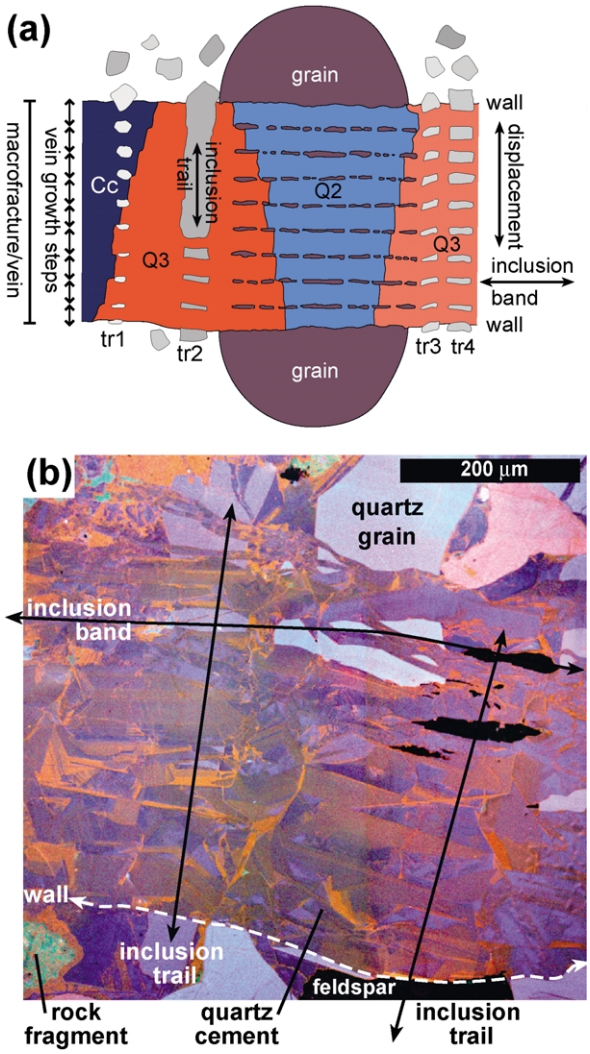

Fig. 1. Features associated with the crack-seal mechanism. (a) Inclusion trails are a series of grain fragments parallel to displacement direction. Fragments of different grains define inclusion bands, which are arranged perpendicular to displacement direction and which formed during the same growth step. Q = quartz, C = calcite, tr = trail. Spacing of inclusion bands is ~50 μm. Modified from Ramsay (1980). (b) Color-CL image mosaic of quartz-lined fracture in sandstone formed by numerous individual crack and cement precipitation events. Quartz grains and cement compose most of the image area; fragmented nonluminescent grain is feldspar, and green speckled areas are rock fragments. Sample is a quartz-cemented lithic arkose, Cretaceous Frontier Formation, Wind River Basin, Wyoming.

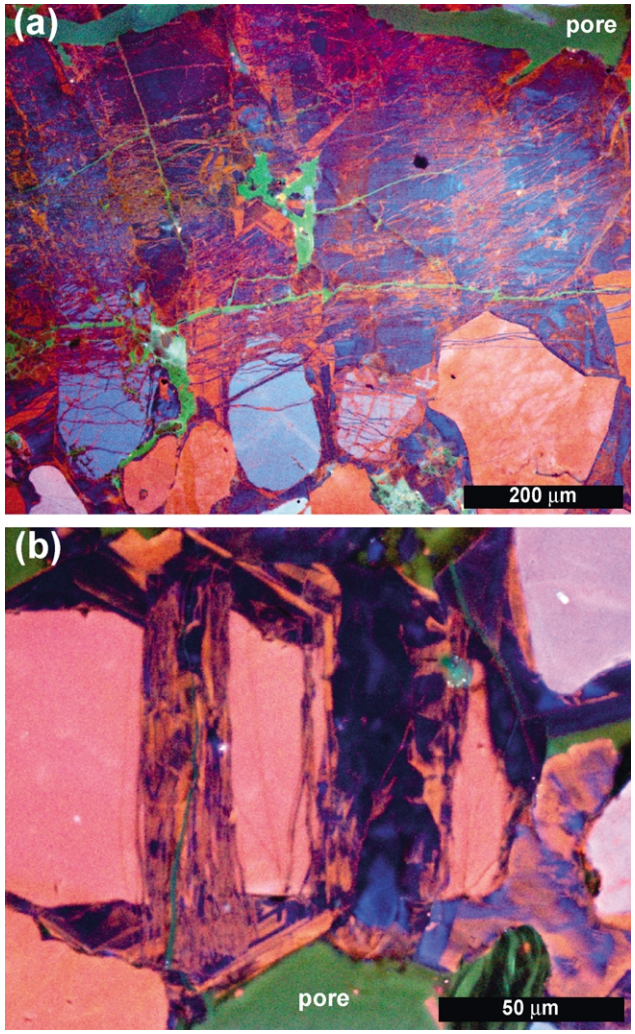

Fig. 2. (a) Color-scanned CL image showing crack-seal texture in a group of quartz bridges and associated fracture porosity. Only one side of the macrofracture is shown; fracture trend is parallel to the long axis of the image. Sample is quartzarenite from a depth of 3009 m. (b) Color-scanned CL image showing post-fracture-opening quartz overgrowths on quartz pillars having central crack-seal texture. Quartz precipitation outlasted fracture expansion. Amount of residual fracture porosity reflects progress of cementation, which depends primarily on thermal history (Lander et al., 2002). In this particular grain, the macrofracture has bifurcated into two strands; overall fracture trend is parallel to the short axis of the image. Sample is a subarkose from a depth of 1865 m. Both samples are from Cretaceous Travis Peak Sandstone, East Texas.

crack-seal textures in an additional 19 formations that range in age from Archean to Tertiary. Samples are mostly from core taken from hydrocarbon reservoirs that have undergone minimal tectonic disturbance. Many samples are from horizontal to gently dipping beds of mostly low to moderate porosity (0–20 bulk volume percent) sandstone. Samples are from rock that is moderately or deeply buried (>1000– ~6200 m) or that has been so in the past. Sandstones are dominantly quartz cemented, although most contain other cements. Quartz cement volumes are typically high (15– >20%), suggesting that host sandstones have been exposed to temperatures more than 80 °C (Lander and Walderhaug, 1999), and fluid-inclusion data from two fracture sets are consistent with temperatures during fracturing of 110 and 240 °C (Laubach, 1989a; unpublished). Rock types include quartz arenites, subarkoses, sublitharenites, lithic arkoses, feldspathic litharenites and litharenites. Grain sizes range from siltstones to granule conglomerates.

The fractures sampled in this study are typical opening-mode (extension) fractures. They are arranged in sets having consistent orientation and are mostly inclined at close to right angles to bedding. Thus, they are nearly vertical in flat-lying beds. More than half the samples are from foreland

basins, and most of the rest are from passive margins and platforms. Foreland samples are from both recent, active basins, such as those of Venezuela, Colombia, Bolivia, and older, inactive foreland basins including the Appalachians, West Texas, and Rocky Mountains. We interpret these fractures to have formed in response to some combination of regional tectonic loading and burial and pore-pressure changes (regional fractures; Nelson, 1985), but it is rarely possible to uniquely relate fracture growth to loading path or to date the fractures. Some fractures in open folds may have formed partly in response to fold-related strains, but other fractures from within fold-thrust belts we interpret to predate folding. In this paper we focus primarily on representative microstructural patterns that are found in fractures in all of these diverse structural settings and ages.

3. Imaging methods

High-resolution microstructure imaging using scanning electron microscope (SEM)-based cathodoluminescence (scanned CL) allows delineation of patterns in fracture microstructure that were previously obscure (Milliken, 1994a; Laubach, 1997; Milliken and Laubach, 2000; Reed and Milliken, 2003) (Figs. 3 and 4). The sensitivity of photomultiplier-based CL systems and the high magnification and stable observing conditions of the SEM significantly enhance weak luminescence. This approach provides an advantage over conventional CL systems in that it allows efficient high-magnification (up to 2000 × imaging) examination of silicate minerals having low levels of luminescence. We obtained digital image mosaics over large specimen areas (square millimeters) and mapped grains, porosity, cement, and fracture patterns. Our survey of sandstone microstructure used more than 325 polished, oriented thin sections and analysis of image mosaics from multiple samples.

The detectors and processing used for these images record CL emissions in the range of 185–850 nm (ultraviolet through visible into near infrared) and convert them to gray-scale intensity values. Most images in this paper were acquired using an Oxford Instruments MonoCL2 system attached to a Philips XL30 SEM operating at 15 kV. We created color images by using red, green, and blue filters and superposing multiple images. Using color filters to convert an originally panchromatic CL source to a synthetic color image commonly reveals textures not evident on panchromatic images. In some samples examined using scanned CL, imaging only part of the available spectrum of CL emissions provides a clearer picture of texture than does using the whole spectrum (Figs. 5a and c and 6). Luminescence variations most likely reflect slight differences in trace-element composition and mineral structure (Pagel et al., 2000). We used contrast between CL colors primarily to document textural patterns. For this application, neither quantitative assessment of emission intensity and color, nor the variables affecting these parameters, are critical.

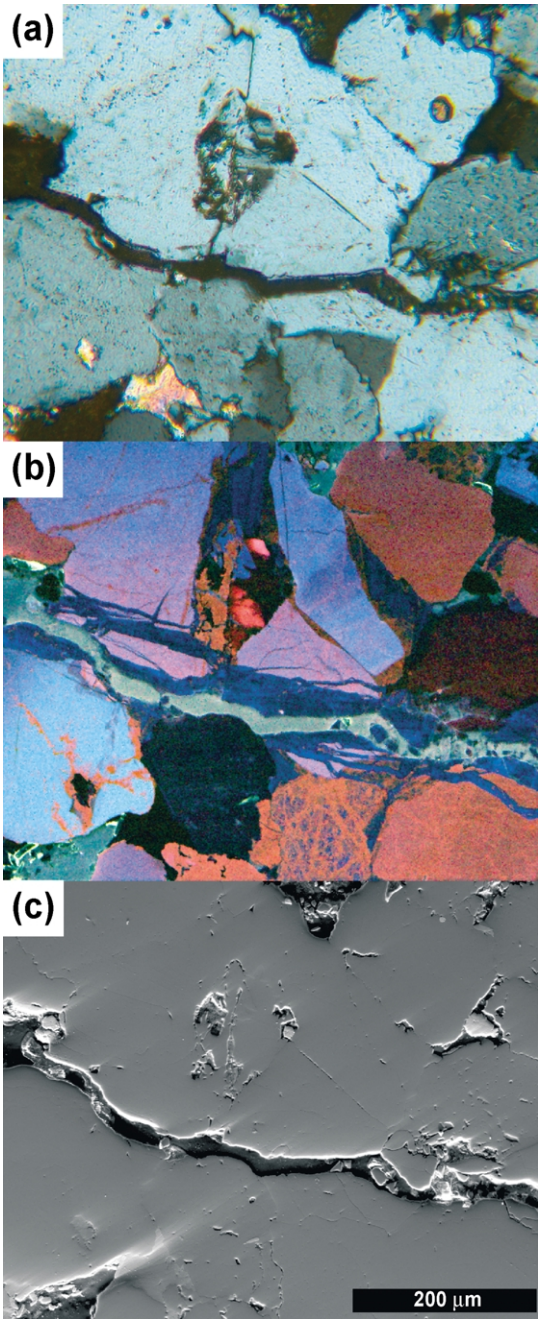

Fig. 3. Image set from a quartz-rich sandstone comparing color CL (center), secondary electron (right), and cross-polarized-light petrographic (left) views. Macrofracture with limited crack-seal texture has been broken during sampling, with reopened area now filled with epoxy. In CL image, fracture-filling epoxy is pale green, quartz grains are blue, red, and purplish red, and quartz cement is dark-blue, black, or red. Calcite cement (an isolated patch in lower-right quadrant) is nonluminescent. Altered feldspar grain in left center shows a patchwork of CL colors. Deformed quartz grain in right center shows a mixture of blue and red luminescence. Microfractures that parallel main fracture are completely filled with blue-luminescent quartz cement. Sample is from Devonian Iquiri Formation, Bolivia.

Scanned CL is a powerful tool for microstructural

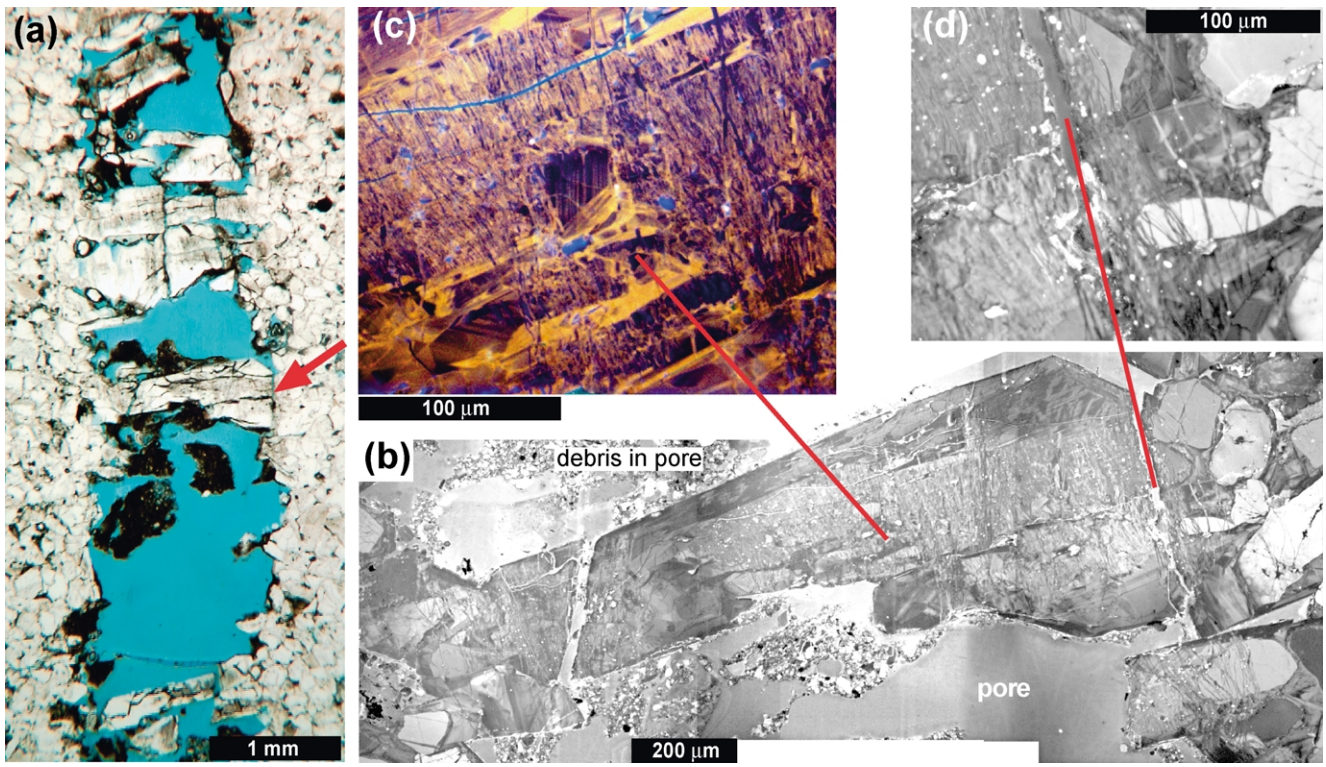

Fig. 4. Relatively simple crack-seal texture, quartz bridge spanning fracture in quartzarenite. Macrofracture strike in all images is identical. Sample depth is 3008.8 m, Cretaceous Travis Peak Formation, East Texas. Macrofracture is near vertical and is associated with subhorizontal stylolites. (a) Plane-polarized-light photomicrograph. Note fracture porosity (now filled with blue epoxy) distributed along fracture length. Red arrow indicates quartz bridge in (b). (b) Panchromatic CL mosaic of entire quartz bridge. Note dozens of smaller fractures that have broken quartz and have been sealed (crack-seal texture). (c) Color-CL image of part of (b); red lines connect corresponding points. (d) Panchromatic-CL image of part of (b), showing the fracture wall, a broken original grain, and the adjacent quartz bridge.

analysis. It provides hitherto inaccessible evidence of crack-seal texture in regional fractures. Applications include identification of cement-filled fringes and shadows around porphyroclasts, fibers in quartz veins in metamorphic rocks (Dietrich and Grant, 1985; Fisher and Brantley, 1992), and fault-gouge and deformation-band textures in sandstone (Fowles and Burley, 1994; Milliken, 1996; Milliken et al., 2004), delineation of grain provenance (Milliken, 1994b; Seyedolali et al., 1997), cement stratigraphy (Hogg et al., 1992), and grain-scale compaction or pressure solution features (Dickinson and Milliken, 1995).

4. Fracture internal structure

4.1. Mineral bridges

The crack-seal mechanism of vein formation has been widely described in low-grade metamorphic rocks and carbonates, mostly from significantly deformed rocks. Crack-seal texture results from repeated opening across a fracture with cement filling in the fracture between increments (Fig. 1; Hulin, 1929; Ferguson and Ganett, 1932; Ramsay, 1980). In contrast to veins in metamorphic rocks, which are commonly filled with mineral deposits, in sedimentary sandstones fractured in diagenetic environments, cements *contemporaneous with fracture opening* rarely completely seal large (aperture >1 mm) fractures. In these rocks, crack-seal texture is commonly found in discontinuous mineral bridges. Bridges are cement deposits that span fractures and that are surrounded by fracture porosity or by later cements (Fig. 4). Fracture volume occupied by bridges can be small and varies from absent to nearly complete fill, with smaller fractures tending to be more completely filled. These mostly inconspicuous bridges hold clear evidence of fracture-widening histories.

In sandstones, crack-seal texture is most common in mineral bridges formed of quartz cement, although examples of crack-seal texture are present in carbonate fracture fills in sandstone as well. The association of localized crack-seal texture (in dolomite cement bridges) and fracture porosity is also present in some dolomites (Gale et al., 2004).

Many quartz bridges have narrow pillar or rod shapes consisting of isolated quartz crystals or masses of crystals. Crack-seal textures occur within these isolated single crystals or clusters of crystals. Some of these crystals show dozens to hundreds of micron-scale, sealed cracks (Fig. 4b). Grain fragments and cement fragments define inclusion bands (Fig. 1) perpendicular to displacement

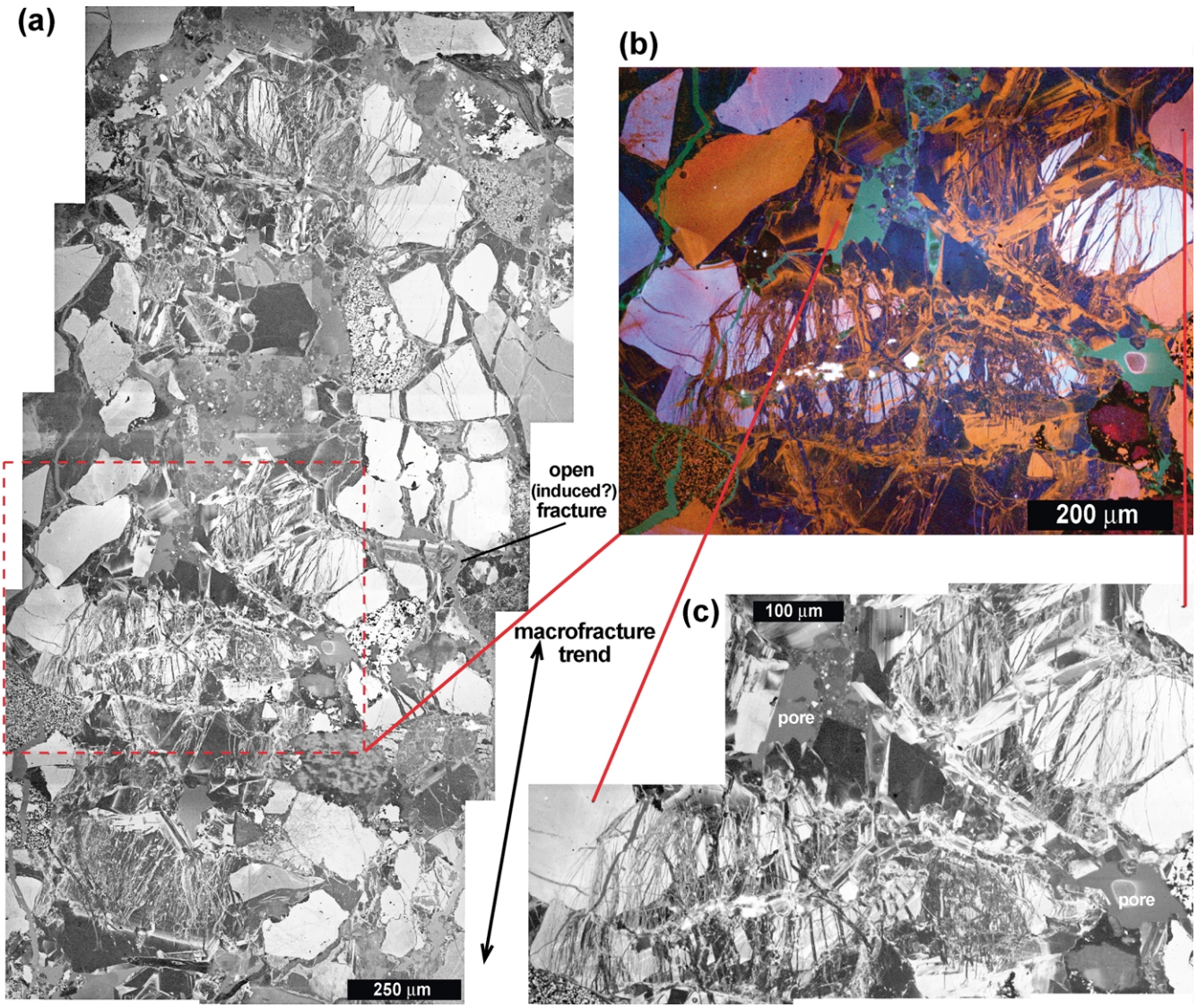

Fig. 5. Complex crack-seal texture within an almost completely quartz-filled fracture. Fracture is parallel to long axis of (a). Sample is lithic-rich, quartz-cemented sandstone of Cretaceous Cozzette Sandstone (Mesaverde Group), from a depth of ~2417 m, Piceance Basin, northwestern Colorado. (a) Gray-scale CL-image mosaic showing segment of fracture. Images represent only CL emissions in the 600– ~ 850 nm range (red to near infrared), an emission range that shows better contrast than a more complete spectrum for this specimen. (b) Color-CL image mosaic of part of (a). Color imaging allows better determination of inclusion trails within crack-seal texture. (c) Gray-scale CL-image mosaic of red to infrared emissions showing detail within (b). (d) Plane-polarized-light photomicrograph of area shown in (a). Red lines connect corresponding points.

direction. Inclusion trails (Fig. 1) form at the boundaries of grain fragments and tend to parallel the wall-rock displacement direction. Continuous-luminescence color bands shown in the CL images probably represent cement that lined or filled fracture porosity following a fracture event. Scanned-CL imaging reveals that many fractures in mineral bridges cut only earlier quartz cement (Fig. 4b). Cement bands associated with these fractures are not marked by inclusion trails, and are nearly impossible to see without scanned CL. Because crack-seal texture is developed in fracture fill that is in crystallographic continuity with grains in bridges and wall rock, in transmitted light these elongate bridges have an appearance that has resulted in their being called *stretched crystals* (Ramsay, 1980).

Within bridges, evidence of repeated fracture includes sharp-sided boundaries, not only between broken grains and cement but also within fracture-lined cement. In many cases, scanned CL reveals micron-scale details of cross-cutting fractures and narrow cement growth zones (Figs. 4 and 5). Individual fractures are commonly less than 1 micron wide.

Crack-seal texture is typically located in the central parts of quartz mineral bridges, although in some examples cement-filled fractures extend to the outer edge of the bridge. A micron-scale veneer of unfractured quartz cement typically surrounds these areas of crack-seal texture (Figs. 2b and 4b). Where this veneer is zoned, filled fractures can be traced various distances across the zoning, apparently

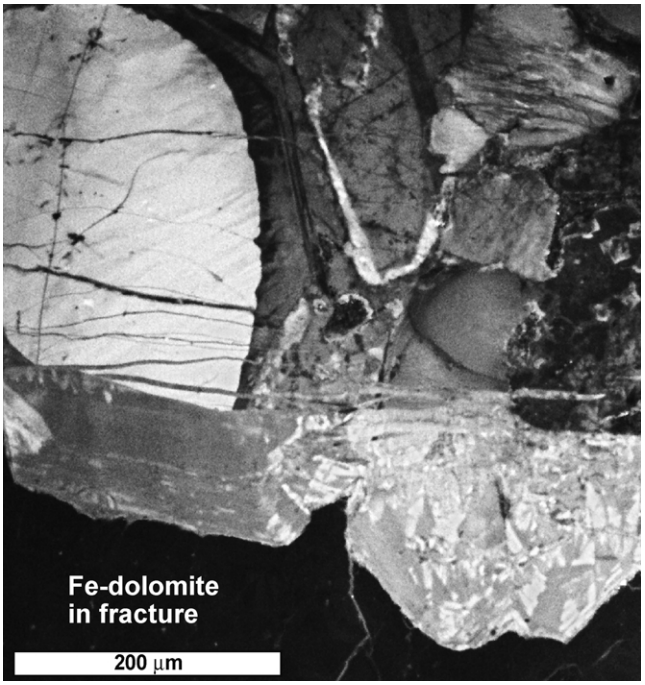

Fig. 6. Limited-wavelength (UV–blue), gray-scale-CL image showing crack-seal texture at the bases of euhedral quartz crystals growing into a macrofracture. Material on the lower part of the image is postkinematic Fe-dolomite cement. Only one side of the macrofracture is shown; opposite side shows similar textures. Sample is from Cretaceous Williams Fork Formation, northwest Colorado. Sample depth is 1748 m. Image by A. Makowitz.

marking cracking and sealing within the bridge, as well as associated euhedral crystal growth on outer parts of the bridge. Where multiple crystals coalesce, complex textural patterns result from juxtaposition of these internal and external bridge textures.

Bridges reflect an unusual cement distribution along fracture walls. Quartz cement contemporaneous with fracture opening (synkinematic cement) is locally much thicker in bridges than in adjacent areas of the fracture. The ratio of cement thickness in mineral bridges spanning millimetric gaps and thin veneers of cements lining fracture walls can be 100:1 or more. Yet quartz cement on fracture walls is comparable in thickness with cement in host-rock pore space.

The concentration of synkinematic quartz cement in bridges leads to many of the features commonly associated with quartz-lined macrofractures. Areas within fractures, but between intact bridges containing crack-seal texture, may be either porous (Fig. 4) or filled to some degree by cement that postdates fracture growth (postkinematic cement) (Fig. 6; Laubach, 1988, 2003). Precipitation in static fractures is typically marked by nonquartz cements surrounding quartz bridges. Textural relations show that crack-seal texture in quartz and porosity developed at the same time. While crack-seal texture was forming in bridges, cement did not fill in fracture pore space in adjacent parts of the fracture. As discussed later, this pattern most likely results from differences in quartz-bridge growth rate relating to substrate and orientation effects (Lander et al., 2002).

Bridges are most common in small, macroscopic fractures (apertures ~1 mm) and in narrow parts of wider fractures. Bridges may be absent because the fracture opened only once (and subsequently filled with cement) or opened sufficiently rapidly that cement never spanned the fracture. In some fractures, bridges are present in narrow fracture segments near fracture tips, whereas central segments may contain only euhedral crystals, presumably because quartz cement precipitation rates were insufficient to bridge the central parts of these fractures during growth (Fig. 7a). However, fractures that lack intact bridges may have relict crack-seal texture near formerly bridged fracture segments, marked by euhedral, terminated quartz crystals having crack-seal texture at their bases (Figs. 6, 7a and 8a).

The amount and location of crack-seal texture visible in a given fracture can be variable. In many cases, evidence of crack-seal processes is subtle and highly localized. Quartz can precipitate in an open fracture undergoing repeated episodic opening without recording crack-seal texture except near fracture tips and in bridges. Subsequent postkinematic cement can fill the fracture, further hiding evidence of contemporaneous deformation and cementation. Such cements will, of course, contain no record of movement. Consequently, along much of their length, many fractures will not show crack-seal texture.

4.2. Substrate effects

Wall-rock composition influences cement and porosity patterns within fractures. Materials in fracture walls that are not favorable substrates for quartz precipitation, such as lithic grains, vacuolized feldspars, and clay minerals, localize residual fracture porosity (Figs. 8 and 9). Thus, for the same fracture and burial history, small fractures in lithic and feldspathic sandstones typically are less completely filled than those in more quartzose sandstone.

Because quartz cement in fractures tends to nucleate in crystallographic continuity with host grains along fracture walls and the orientation of these grains varies, the local substrate crystallographic orientation can play a role in the details of bridge growth (Figs. 7a and 9c). An example from the Cretaceous Frontier Formation shows a quartz-lined macrofracture (Fig. 9) having four quartz grains hosting whole or partial quartz bridges, which contain dissimilar crack-seal textures. The dissimilarities result at least partly from differing growth rates along different crystallographic axes in quartz (most rapid growth is parallel to the *c*-axis).

4.3. Patterns of crosscutting fractures

Crosscutting fracture patterns (Fig. 9b) are potentially significant guides for unraveling linked mechanical and cementation history. An example from Permian

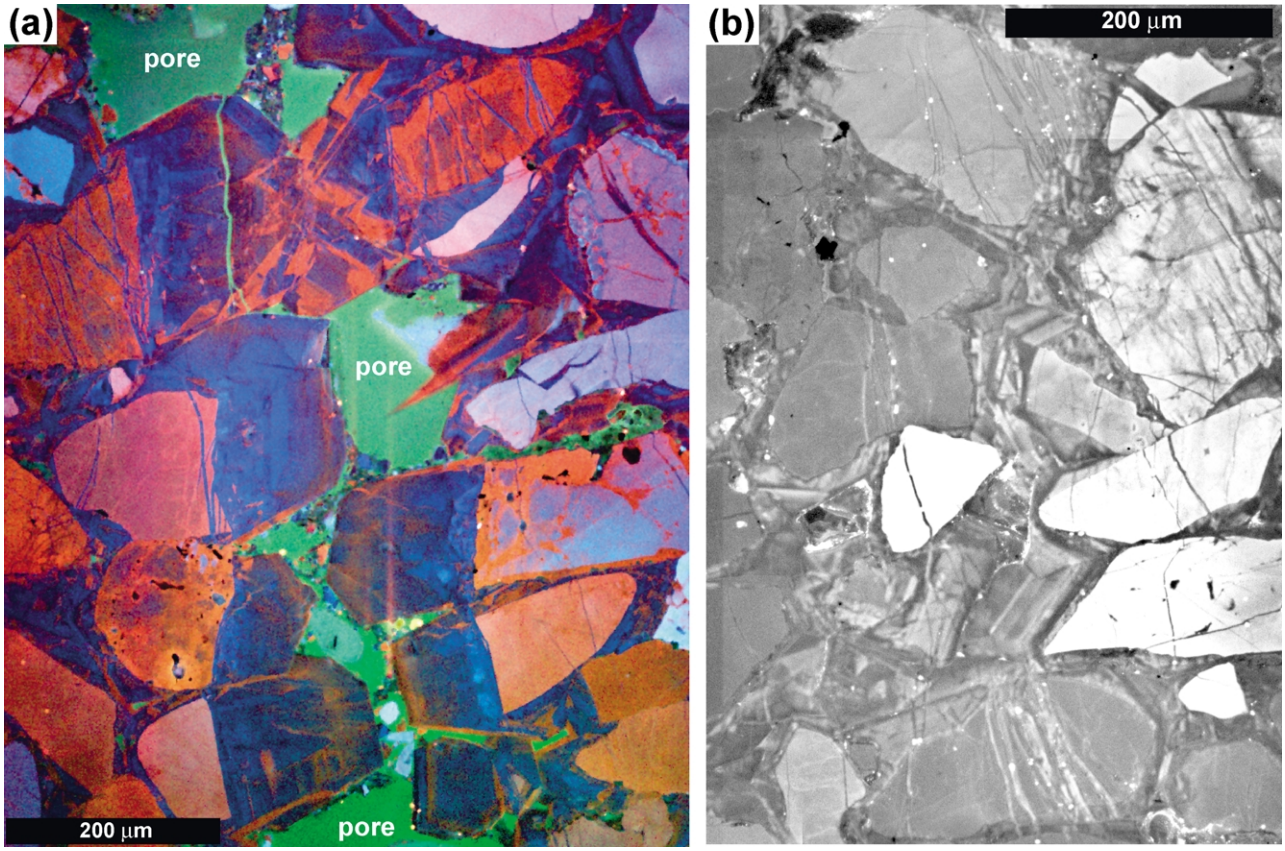

Fig. 7. Comparison of textures in central area of fracture with textures near fracture tip. Macrofracture trend is parallel to the long axis of the images. (a) Color-CL image from center of a macrofracture. (b) Panchromatic-CL image mosaic of fracture tip from same macrofracture. Image areas are approximately 12 mm apart. Both images show crack-seal texture, but note increased porosity and prevalence of unfractured, zoned, euhedral quartz in color-CL image from center of macrofracture (a). Sample is a quartz-cemented quartzarenite, depth 3008.8 m, Cretaceous Travis Peak Formation, East Texas.

Wolfcamp Formation (Fig. 10) shows that in this fracture, initial cement growth was euhedral, mostly blue-luminescent, quartz cement. These crystals were cut by a set of fractures filled by orange-luminescent quartz cement. The change in cement reflects a change in precipitation conditions between early and late in the growth of the fracture.

Crack-seal patterns commonly vary along fracture traces and from one bridge to the next. These patterns mark interplay between incremental fracture widening and patterns of crystal growth into fracture cavities (Fig. 9b, #12). Some patterns, such as blunt fracture ends of quartz-filled fractures at CL-zone boundaries (Fig. 9b, #1), mark areas where porosity existed at the time fractures formed but that was subsequently destroyed by continued cement precipitation. Some structures reflect interference of simultaneous crystal growth from opposite sides of a fracture (Figs. 7a and 9b, #5).

In sandstones, fracturing occurs in both syntaxial and antitaxial positions, and these patterns may be mixed within the same fracture set or even the same fracture. Thus, in quartz bridges, fracturing is commonly ataxial, with new fracture increments forming sequentially at various points throughout existing fracture fill (at different points within a bridge). Bridges combine aspects of both syntaxial and antitaxial fibers. Syntaxial fibers grow in optical continuity from grains in fracture walls and meet at a central seam, with the oldest parts of fibers adjacent to fracture walls. Antitaxial fibers grow incrementally from cement fill into fracture walls, lack a central seam, and are not continuous from wall grains with the youngest parts at fracture walls (Dunne and Hancock, 1994). From one quartz bridge to the next, fracture locations in bridges may be inconsistent (Figs. 5a, 8 and 9); care is thus needed in interpreting crack-seal history from fluid inclusions using optical microscopy. Scanned-CL imaging reveals that wall-rock inclusions within adjacent bridges that line up do not necessarily mark the same growth step.

In some fractures that have fills formed by the crack-seal mechanism, there is a gradation inward from closely spaced microfractures in fracture walls, to highly fractured wall-rock and cement zones, to massive, less fractured fill within fracture centers (Figs. 2a, 4d and 7a). This pattern probably results from cement precipitation, where cement initially spans a narrow fracture, but for the subsequent wider fracture the cement occurs without spanning the gap.

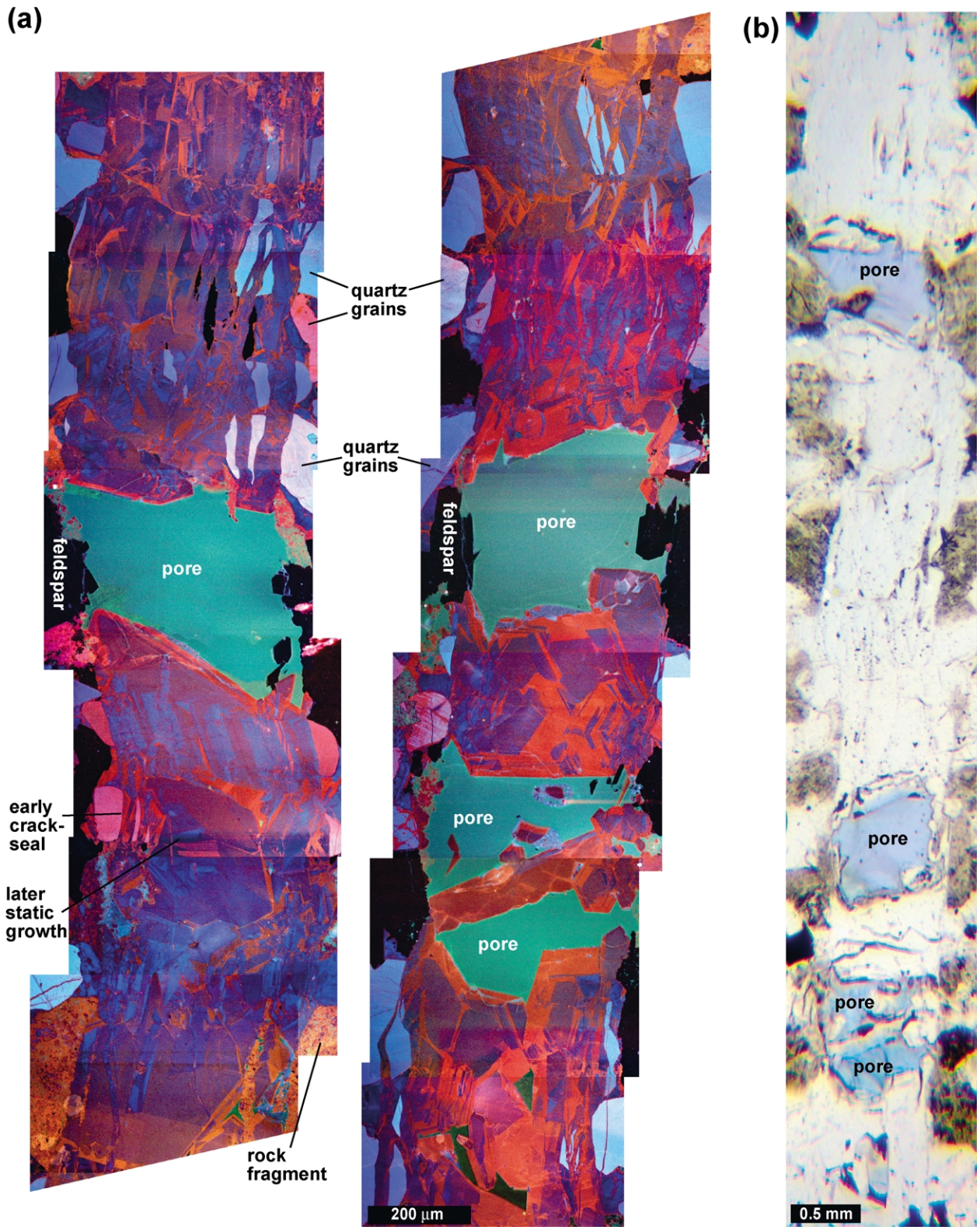

Fig. 8. Images showing variability in fracture structure along fracture plane. (a) Color-CL image mosaic along a partly open, quartz-lined macrofracture. Mosaic has been split; left image connects to the top of the right image. Bright-green, luminescent, epoxy-filled porosity is associated with nonluminescent feldspar grains. Quartz bridges adjacent to one another do not necessarily show the same patterns of breakage. (b) Plane-polarized-light photomicrograph mosaic of macrofracture shown in (a). Image shows approximately the same macrofracture area as (a). Brown grains are altered feldspars and rock fragments. Sample is lithic arkose from 6244.6 m, Cretaceous Frontier Formation, Wind River Basin, Wyoming.

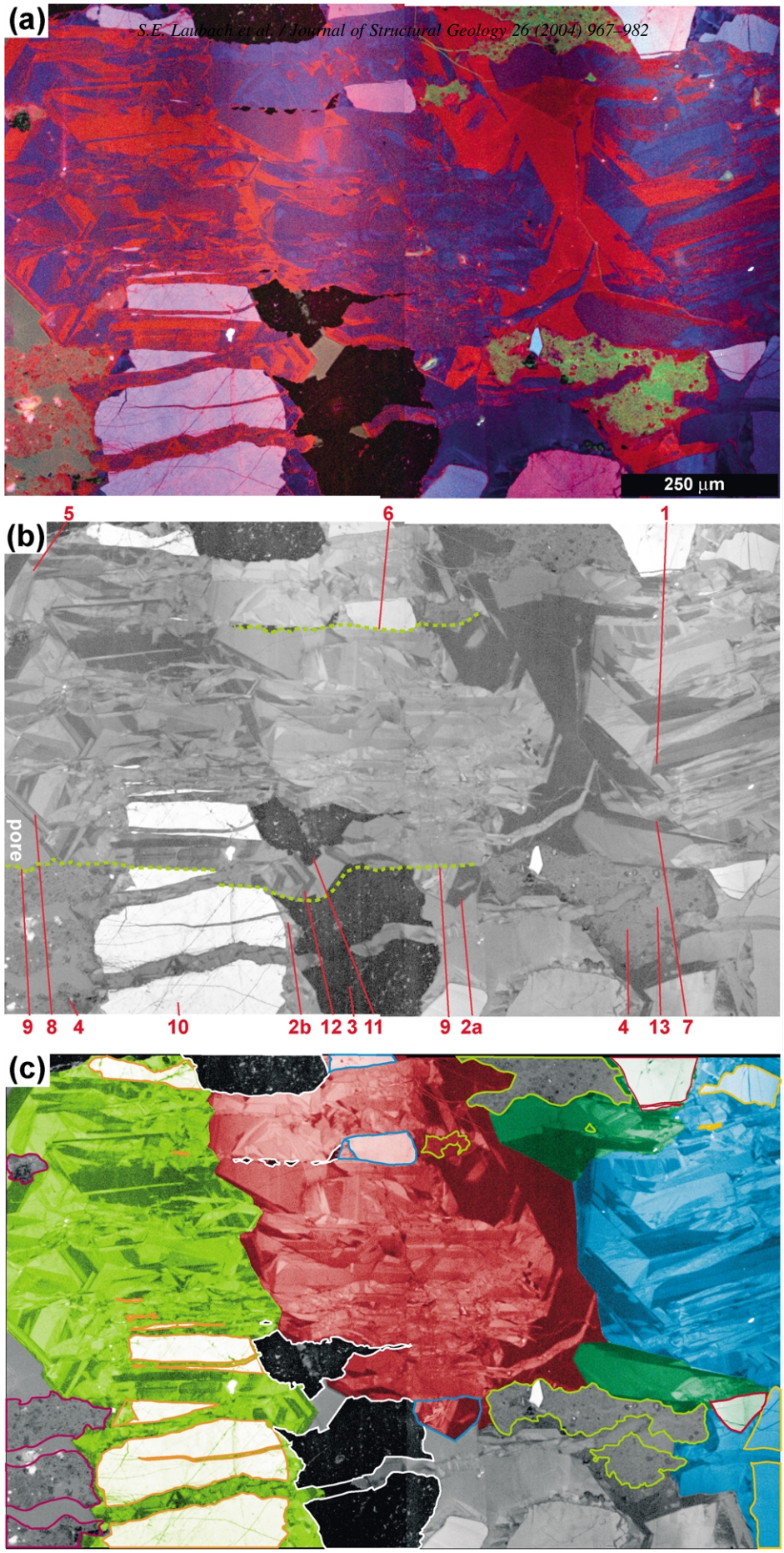
(a)
250 μm
(b)
5
6
1
pore
9 8 4
10
2b 12 3 11
9 2a
4 13 7
(c)

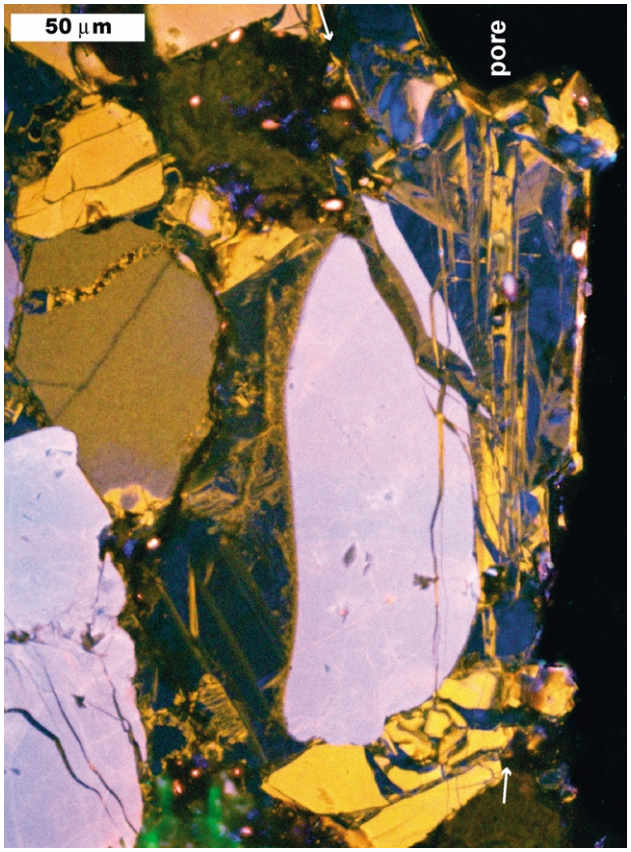

Fig. 10. Color-CL image showing one side of macrofracture rebroken during sampling. Overall macrofracture trend is parallel to the long axis of the image; arrows mark approximate fracture walls. Polyphase fracture-lining quartz cement is defined by different luminescent colors. Euhedral, mostly blue-luminescent, quartz cement in fracture is cut by incremental fractures filled with orange-luminescent quartz cement. Sample is a quartz-cemented sandstone from Permian Wolfcamp Formation, Val Verde Basin, West Texas; depth 2516.7 m.

4.4. Fracture tips and links

Tips of macrofractures in sandstone and areas of fracture overlap and linkage show intersecting and overlapping fractures that resemble crack-seal texture formed within the main parts of fractures. These zones of fracture growth and coalescence produce distinct varieties of crack-seal texture.

Although many fractures merely taper to a tip, near their tips some fractures die out by transforming into swarms of microfractures. Transcement or transgranular, quartz-lined microfractures are common at fracture tips (Fig. 7b). These microfractures may constitute fossilized process zones (Labuz et al., 1987). When the main fracture grows past these microfractures, they appear as a type of crack-seal texture.

Both crack-seal texture and within-fracture quartz cement tend to be more common near tips than in centers of macrofractures (Fig. 7). In many cases, the center of a macrofracture will show only early-stage crack-seal texture and euhedral quartz crystals, but fracture tips will have full-span quartz bridges that show crack-seal texture. Crack-seal texture can form only where cement can span fracture gaps before the next increment of fracture growth, so this pattern is probably a result of incomplete cement failing to span the widest parts of fractures during incremental crack growth (Fig. 7).

Some microfracture arrays near fracture tips are arranged in divergent fans of crosscutting, superposed microfractures localized at fracture tips but not elsewhere along fracture walls, as might be expected for bypassed process zones (Laubach, 1989a). Each growth increment and accompanying expansion of the main fracture result in a new quickly sealed microfracture extending away from the main porous section of the main fracture. The fracture lengthens but subsequently shortens owing to cement deposited in fracture

Fig. 9. (a) Color-CL image mosaic of a quartz-lined macrofracture. Quartz grains and euhedral overgrowths partly filling fracture were broken repeatedly by later fracture increments. Green speckled areas within fracture are epoxy-filled fracture porosity. Macrofracture trend is parallel to the long axes of the image. (b) Panchromatic, gray-scale-CL image mosaic of same area as in (a), but labeled to show important features. (1) Note blunt termination of this quartz-filled fracture at a CL-zoning boundary. At the time the fracture formed, the blue-luminescent band was at the edge of a euhedral crystal bordered by porosity. The red-luminescent cement band grew after the fracture formed and filled. (2) Prekinematic quartz overgrowths are generally euhedral (pore-filling) and show zoned, mostly blue luminescence. 2A is an overgrowth that has been broken off its grain (see quartz grain at 6); 2B is still attached to grain on which it grew. (3) Detrital feldspar grains are not typically nonluminescent, as these are, unless they have undergone significant alteration. Authigenic feldspar cement (see 11) is typically nonluminescent. (4) Rock fragments in this sample have intermixed red and green luminescence in color CL. Green luminescence is due to epoxy filling microporosity within grain. (5) Dovetail shape defined by CL-zoning, a result of simultaneous euhedral quartz growth from both sides of a fracture meeting in the center. These structures help unravel the complex history of this macrofracture. This fracture increment occurs entirely within quartz cement, which fills a larger fracture. (6) An inclusion band defined by (top to bottom) a rock fragment, part of a quartz grain, fractured prekinematic quartz cement, and a trail of small nonluminescent feldspar grain fragments. This band marks the boundary between two microstructural provinces inside a larger macrofracture and is possibly one side of the earliest fracture increment. (7) Quartz crystallographic boundary that is also a boundary between quartz bridges with different mechanical histories. Fracture fill shown here includes four different quartz crystallographic domains, three of which span the macrofracture (Fig. 12). (8) Unfractured, late euhedral cement growing into a pore. (9) Partial trace of an early fracture surface that cuts grains and prekinematic cement but not synkinematic cement. This trace is cut by at least one later fracture. (10) Fractured quartz grain, which contributes at least seven pieces to an inclusion trail. (11) Euhedral outer zones (nonluminescent) growing into fracture porosity represents cryptic authigenic feldspar cement associated with host feldspar grains. (12) Euhedral quartz cement that grew laterally into fracture porosity adjacent to a broken feldspar grain. (13) Pore-filling epoxy typically has a speckled green luminescence in color CL. In this case, epoxy is the filling microfracture porosity inside a rock fragment. Sample is a feldspathic litharenite from the Cretaceous Frontier Formation, Wyoming, depth 6242.15 m. Thin section cut parallel to bedding. (c) Limited wavelength (ultraviolet to blue), gray-scale-CL image having other superimposed information. Margins of original sedimentary grains are outlined in a different color for grain fragments making up each inclusion trail. Color tinting delineates four optically continuous areas of quartz (areas include both grain and overgrowth cement).

tips. This pattern is a type of crack-seal texture we infer to be associated with stationary crack tips. Macrofractures associated with this style of crack-seal texture tend to be unusually wide relative to their heights, having height-to-width ratios of less than 200 (Laubach, 1989b). This pattern implies feedback between cement precipitation, fracture growth, and possible decay of stress perturbation around the main fracture. Perhaps the right loading, temperature, and fluid conditions result in fracture systems that *stall*.

Evidence of repeated fracture and cementation is found where en échelon fractures link or overlap. Microfractures are common where en échelon macrofracture strands overlap (Fig. 11). Microfractures in the overlap region connecting large fracture segments can link and amalgamate into a single continuous macrofracture. Along large fractures, previous areas of overlap fossilize a variety of crack-seal textures representative of fracture linkage (similar to *vein coalescence*; Misik, 1971).

Multigenerational fracture growth near an en échelon step between two macrofractures in Cretaceous Fall River Sandstone core (Johns et al., 1995) shows in plan view early microfractures obliquely spanning the step between tips of large fractures (Fig. 11). These microfractures are crosscut by later microfractures aligned parallel to the macrofracture trend that record a growth history in the zone surrounding interacting crack tips. The transition from curved to straight traces could result from increased far-field fracture-parallel compressive stress during fracture growth (Olson and Pollard, 1989).

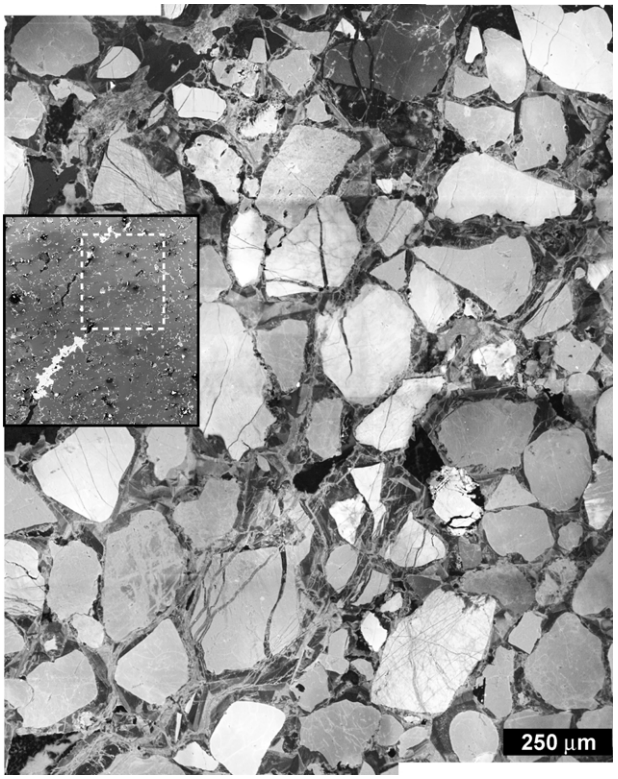

Fig. 11. Panchromatic, gray-scale-CL image mosaic showing transcement or transgranular, linking quartz-lined microfractures in the overlap zone between two macrofractures. Most visible grains are quartz. Inset shows a secondary electron image of the overlap zone; dashed square marks the approximate area of the CL mosaic. In the macrofractures, early synkinematic quartz cement is followed by postkinematic barite cement (light-colored in secondary electron image), which has partly filled the fracture porosity. Inset image is ~5.1 mm wide. Sample is a quartz-cemented quartzarenite of the Cretaceous Fall River Formation from the Powder River Basin, Wyoming. Sample depth is 3774.9 m.

4.5. Variations in extension direction

Crack-seal texture can record evidence of (1) changes in incremental extension direction during deformation and (2) extension oblique to strike of the incremental fracture (Fig. 12). These are mostly examples of ataxial, as opposed to syntaxial or antitaxial, incremental fracture patterns. Graphic restoration of grain fragments in some cases shows that changes in overall extension direction are small despite changes in orientations of fracture-forming growth increments through time (Fig. 12a). However, markedly differing early and late incremental extension directions are locally evident, including one example (Fig. 12b), where the late direction differs by 65° from the early direction. In our data set, both progressive changes in extension direction and reactivation of fractures during later, separate fracturing events are attested.

Although most examples have simple patterns of opening normal to fracture walls, we have also found rare examples of textures that have a chaotic appearance compared with that of typical crack-seal texture. An example from within a fracture from the Weber Formation (Fig. 13) has grain fragments that were apparently plucked from the walls but rotated before sealing. How this structure evolved is obscure. However, this structure, and previous examples with simpler patterns, illustrates the potential for CL to track complex, kinematically significant structural patterns within quartz bridges.

4.6. Crack-seal texture in microfractures

In addition to large fractures, crack-seal texture is present in microfractures (Fig. 14). A few micron-scale microfractures have distinct crack-seal texture, indicating many increments of fracture opening. In general, however, microfractures of this size and smaller tend to be sealed and to lack distinct crack-seal texture. This situation may partly reflect the fact that these fractures are many times smaller than particles in host sandstone, making entrainment of distinct wall-rock fragments unlikely. In many cases, resolution limits of scanned CL hinder delineation of crack-seal texture in cement at this magnification. Crack-seal texture is documented in microfractures but is frequently obscure.

A spectacular example of fine-scale, crack-seal texture from the Pennsylvanian Pottsville Formation shows five to seven increments of opening in a fracture only about 35 microns wide (Fig. 14b). Microfractures of this size and

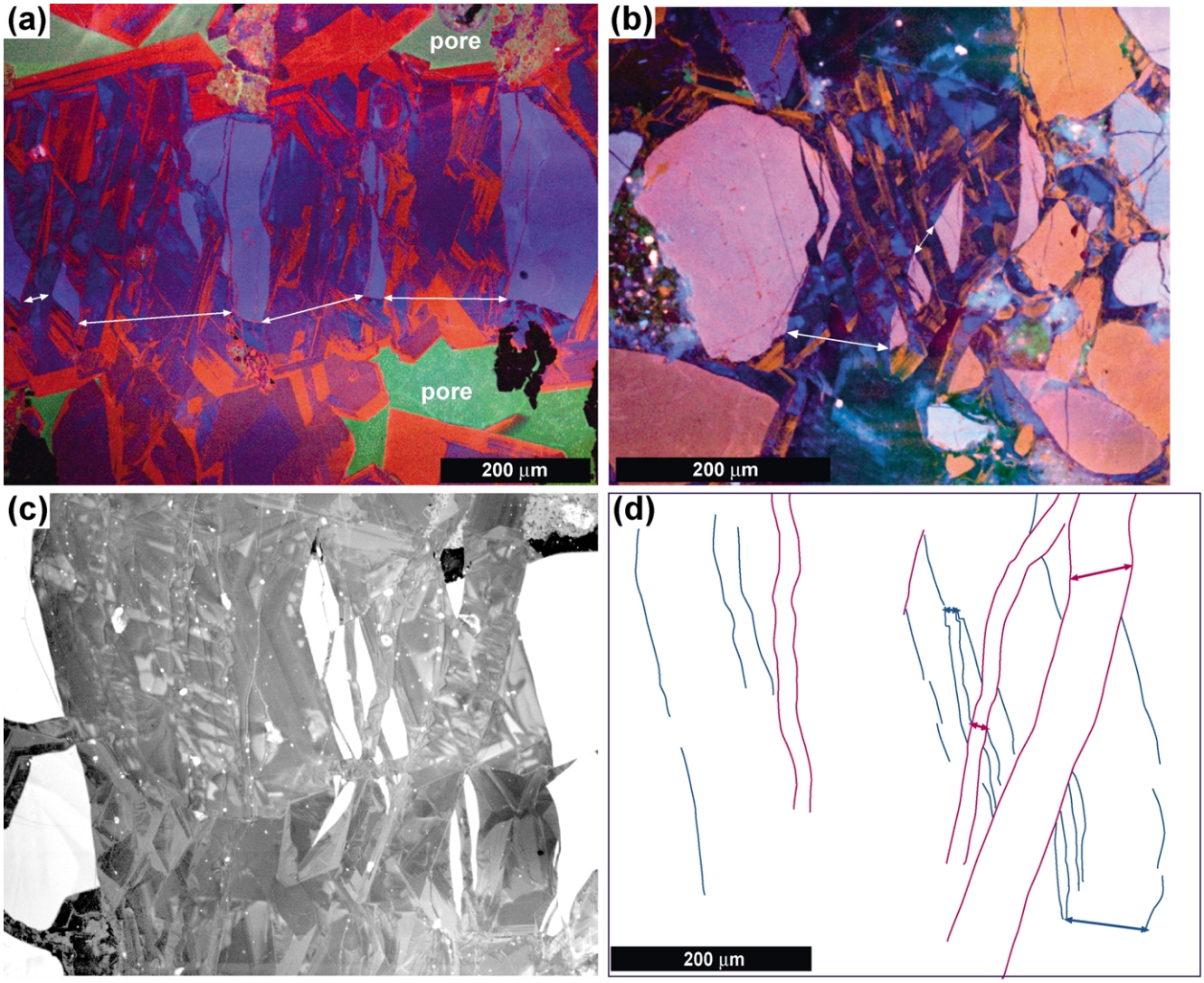

Fig. 12. Apparent variations in extension direction marked by progressive shift in fracture trends and cement-growth increments. In each image, overall fracture trend is roughly parallel to the short axis of the image. (a) Color-CL image showing crack-seal texture in a quartz bridge; reconnection of grain fragments suggests that extension direction (arrows) has not changed markedly, although the trends of early and late fractures are different. Feldspathic litharenite from Cretaceous Frontier Formation, Wyoming; 6242.1 m. (b) Fractured quartz bridge (center) surrounded by almost nonluminescent postkinematic carbonate cement. Early and late incremental extension directions differ. Color-CL image, of a sublitharenite from Permian Wolfcamp Formation, Val Verde Basin, West Texas; depth of 2386.4 m. (c) Small fractures within larger fracture showing that displacement direction of crack-seal opening steps changed with time. Panchromatic, gray-scale-CL image. Lithic arkose from Cretaceous Frontier Formation, Wyoming; depth 6244.6 m. (d) Line drawing delineating extension directions in (c). Early fractures are outlined in blue; late fractures in purple.

smaller tend to be sealed or to have only small, discontinuous areas of porosity. Where visible, extension increments of microfractures having crack-seal texture are commonly on a submicron scale.

Progressive microfracturing and crosscutting relations among cement zoning and microfractures in host rocks also record fracture-timing information relative to cement precipitation. Microfractures that are distant from large fractures, yet are aligned with them and contain cement of the same relative age, are common (Fig. 6), suggesting that both are responding to the same far-field loads (Laubach, 1997). Moreover, consistent size distributions ranging over several orders of magnitude (Marrett et al., 1999) suggest that these disseminated microfractures are smaller versions of the fractures that contain crack-seal texture.

5. Discussion

5.1. Conditions leading to crack seal in sedimentary rocks

In folded and faulted sandstones, crack-seal texture is unsurprising because the large forcing structures probably grew incrementally. Where crack seal has been identified in sedimentary rocks, examples are mostly from fault zones (Anders and Wiltschko, 1994), although a few examples

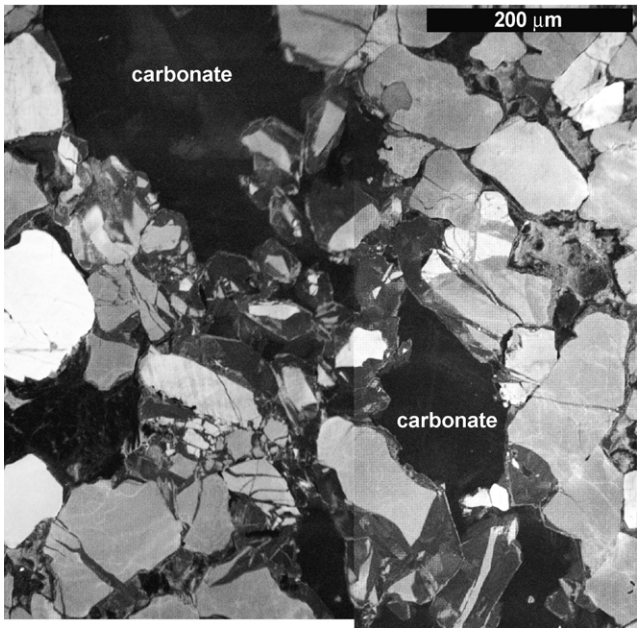

Fig. 13. Panchromatic, gray-scale-CL image showing an apparently chaotic crack-seal texture within a macrofracture, Pennsylvanian–Permian Weber Formation, Rangely field, Piceance Basin, Colorado. Grain fragments located within fracture have been torn from walls and rotated prior to sealing. Least luminescent material in macrofracture is Fe-bearing carbonate cement that surrounds and postdates euhedral quartz overgrowths. Sample depth 1738.2 m.

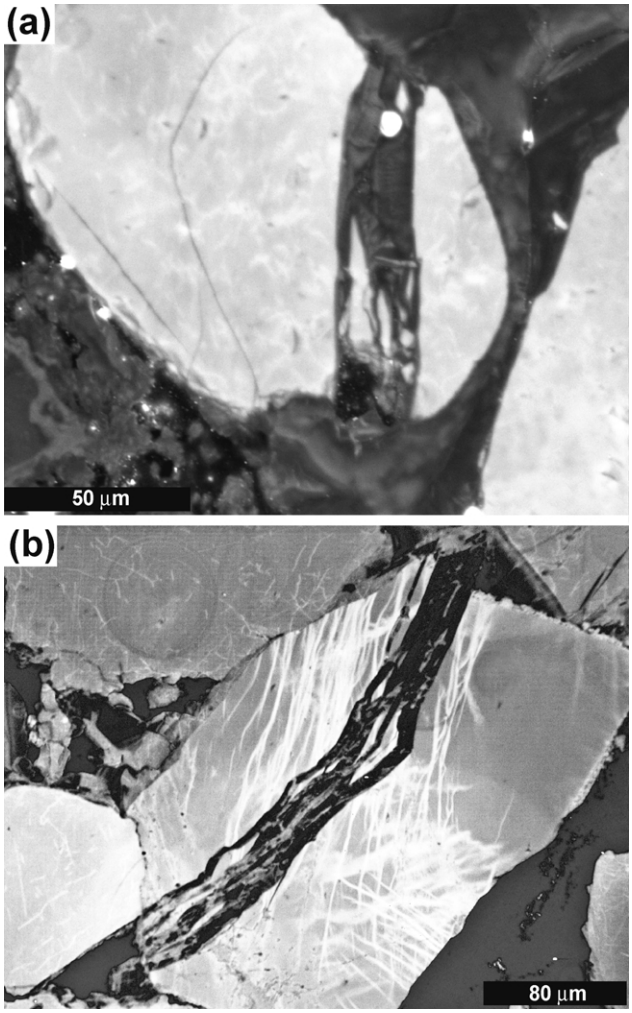

Fig. 14. Crack-seal texture in microfractures. (a) Panchromatic, gray-scale-CL image of sample from Cretaceous Dakota Formation, San Juan Basin, New Mexico; depth 2154.4 m. (b) Panchromatic, gray-scale-CL image of sample from Pennsylvanian Pottsville Formation, Black Warrior Basin, Alabama; depth 1052.5 m. Brightly luminescent linear structures in quartz grain are probably a result of plastic strain. Round structure in upper left is an imperfection in sample preparation.

were described in relatively undeformed rocks (Laubach, 1988). Our study shows that crack-seal texture is common in horizontal to subhorizontal sandstone beds distant from faults or folds, if sandstones have been subject to burial sufficiently deep and protracted for quartz cement to precipitate. These structures have never been imaged as unambiguously as they are using scanned CL. In many samples, the only structures associated with crack-seal texture are the host fractures with their flanking microfractures, and, in some cases, bed-parallel stylolites. The conditions leading to crack-seal texture must therefore be prevalent in regional fractures under a wide range of burial conditions and tectonic settings.

Qualitative evidence suggests that internal structures in fractures vary to some extent with burial depth and location. For example, fractures formed in deeper, better cemented rocks, tend to cut through, rather than around, grains and, hence, show more complex internal structures. Increased burial depth generally correlates with increased temperature and increased quartz precipitation, which can lead to better developed, more complex bridges.

In two areas where we have analyzed primary fluid inclusions trapped in cements associated with crack-seal texture, a range of temperature and salinity values is evident. Saline fluid inclusions having mean temperatures of about 110 °C but a range of more than 50 °C are present in crack-seal structures in East Texas sandstones at about 3000 m (e.g. Laubach, 1989a,b; Lander et al., 2002) and low-salinity fluid inclusion having bimodal trapping temperatures of 140 and 230 °C and ranges of more than 25 °C occur in crack-seal structures in Wyoming at about 6000 m (Laubach, unpublished). These results show that a wide range of burial conditions or fluid temperatures can be associated with quartz bridges having crack-seal texture and associated fracture porosity.

Crack-seal texture is associated not only with precipitation of quartz cement but also preservation of fracture porosity for fractures of a specific size and larger. This association suggests that for the burial histories and time of fracturing of the rocks that we examined, the rate of cement precipitation for quartz is insufficient to occlude fracture porosity after fractures formed. Textures on the margins of bridges show that quartz precipitation did not stop when fracture opening ceased. Because the samples we studied represent a wide range of current burial depths and burial histories, bridging and crack-seal textures are unlikely to

result from basin-specific or rarely developed diagenetic conditions. Likewise, unusual structural conditions are probably not responsible for these structures. Repeated fracture opening marked by crack-seal texture and other evidence of episodic fracture growth, such as arrest lines, is consistent with natural hydraulic fracture mechanisms of fracture growth (Laubach, 1988; Engelder and Fischer, 1996). Such structures can arise under a wide range of tectonic, burial, and pore-pressure histories.

Crack-seal texture may be frequently associated with quartz cement precipitation in moderately to deeply buried sandstones because throughout much of a sandstone's burial history, substrate composition and rock-dominated fluid chemistry dictate that this cement is most likely to precipitate. Diagenetic modeling and high-temperature precipitation experiments show that bridges most likely result from rapid crystal precipitation on repeatedly renewed fracture surfaces (Lander et al., 2002). Multiple fracture events are required to create bridges, and the rate of fracture growth cannot greatly exceed cement precipitation rate. The size of bridges and constituent cement layers within crack-seal increments most likely depend on the time/temperature history of the fracture, the primary controls on cement precipitation rates and volumes, and fracture-opening rates. Used in conjunction with diagenetic-modeling and burial-history information, the ratio of fracture to host-rock cement volume is a potentially important metric of deformation history (Lander et al., 2002).

Because quartz frequently does not fill large fractures even in deeply buried sandstones, these structures may become cemented by other phases such as carbonate minerals. The rarity of crack-seal texture in carbonate fracture fills in sandstones suggests that mechanical conditions leading to fracture growth infrequently coincide with geochemical conditions favoring carbonate mineral precipitation in these quartzose rocks. For many types of sandstone, fluids associated with fracture growth are the same as those that precipitate quartz cement, suggesting that these are the fluids that are relevant to subcritical crack growth (cf. Holder et al., 2001).

5.2. Evidence against force-of-crystallization vein growth

The interpretation in the previous section contrasts with models of vein formation where vein and fracture growth are different processes. For example, Wiltschko and Morse (2001) assumed that veins are characteristically completely filled with cement and proposed that cement-filled veins are consistent with vein widening caused by pressure due to growing crystals. They suggested that some veins originate at sites of precipitation and then widen because of pressure exerted by crystal growth. As materials precipitate, vein walls are pushed apart. In their scenario, a nonzero remote differential stress is proposed to explain vein alignment. Resulting veins have shapes typical of opening-mode cracks except that, mechanically, crystallization pressure replaces the role of internal fluid pressure in their propagation. Veins that formed by this mechanism involve precipitation forces driving crack growth. These researchers ascribed apparent crack-seal texture to geochemical self-organization at the vein wall driven by pressure–solution-enhanced supersaturation in pore fluid and nonlinear precipitation kinetics at the vein wall.

Sharply defined wall-rock fragments and fractured cements in narrow cement bridges are compelling evidence that cement crystallization did not drive fracture growth in the examples we studied, even though some of these fractures are now filled with cement (i.e. they are veins). The association of clearly delineated crack-seal texture and increasing fracture porosity with increasing fracture size shows that cement fills fractures passively, responding to the growing crack rather than driving it. Narrow-diameter bridges of vein-fill material having crack-seal texture are incompatible with models of fracture growth that call on cements to push fracture walls apart and call for apparent crack-seal textures to reflect geochemical self-organization. Vein-filling carbonate cements in the sandstone samples we examined are typically deposited *after* fractures ceased widening (Laubach, 2003). The force-of-crystallization mechanism for vein expansion (Wiltschko and Morse, 2001) is not a viable explanation for these widespread, open or mineral-filled fractures.

5.3. Implications for fracture growth modeling

Where regional opening-mode fractures are unrelated to faults and folds, crack-seal texture marks episodic fracture growth driven by interplay of evolving rock properties, compaction, pore pressure, burial-related temperature changes, and overburden and remote tectonic loads. Some combination of increased fluid pressure, decreased confining stress, and subcritical crack propagation is probably responsible for driving fracture growth (Engelder and Fischer, 1996; Olson et al., 2001). In these settings, cementation-related pore-pressure change is a possible mechanism for overpressure generation (Bjørkum and Nadeau, 1998; Lander et al., 1999; Walderhaug et al., 2001; Wangen, 2001). Crack-seal textures and evidence of cement accumulation rates could clarify whether local transient pore-pressure increases, associated with rapid cementation, could be a driver of fracture growth.

Together with temperature, burial history, and mineral kinetics information, crack-seal textures could provide evidence to constrain fracture-opening rates (Lander et al., 2002). By studying growth histories of individual fractures in a population and tying growth history to cement stratigraphy and other geochemical information (e.g. fluid inclusion temperature and pressure data), we can place the evolution of fracture arrays in the context of thermal and burial-history models and numerical models of fracture growth (Lander et al., 2002; Olson, 2004). These structures

could provide a useful link between mechanical and diagenetic modeling. Although the mechanics of natural opening-mode fractures has been extensively debated (Hancock, 1985; Pollard and Aydin, 1988; Engelder and Fischer, 1996; National Research Council, 1996), the potential for diagenetic reactions in fractures to influence fracture mechanics has not been widely appreciated, aside from the phenomenon of subcritical crack propagation (Atkinson, 1984; Holder et al., 2001). To the extent that cementation influences changing rock and fracture properties and pore-fluid pressure, comprehensive models of fracture systems need to account for both mechanical and chemical/cementation processes.

6. Conclusions

Crack-seal texture is present in isolated mineral bridges surrounded by fracture porosity for a wide range of sandstone rock types, tectonic settings, and burial depths. These structures document episodic fracture growth that can include tens to hundreds of growth increments in regional opening-mode fractures having apertures of a few tens of microns to several millimeters or more.

Linked crack-seal texture, bridges, and fracture porosity reflect competition between fracture growth and cement precipitation. Bridge formation probably reflects competition between fracture opening rates and cement accumulation rates (Lander et al., 2002). Most fractures never achieve the size or opening rate critical to outstripping cement precipitation and, therefore, cease growing and become sealed. As fractures widen, cement can no longer grow across open parts of the fracture before the next fracture-growth increment. Cement precipitation that falls far behind fracture expansion leads to wide, mostly open fractures having thin veneers of quartz on fracture walls. Because this association of structures is present in a range of settings, it is not the product of unique circumstances in burial history and fluid flow. We interpret them to reflect the confluence of rock-dominated geochemistry that is widespread in time and space and fracturing caused by a spectrum of loading conditions. The fine detail of cement accumulation in crack-seal texture visible using scanned CL has great potential for helping to unravel the operation of these linked diagenetic and structural processes.

Acknowledgements

Partly supported by a grant from the Office of Basic Energy Sciences, U.S. Department of Energy, Contract No. DE-FC26-00BC15308 and by industrial associates of the Fracture Research and Application Consortium: Chevron-Texaco, Devon Energy Corporation, Ecopetrol, Marathon Oil, PEMEX Exploración y Producción and IMP, Petroleos de Venezuela, Petrobras, Repsol-YPF, Saudi Aramco, Shell International Exploration & Production, Schlumberger, Tom Brown, Inc., and Williams Exploration & Production. We are grateful to associates for sample suites used in this study, to A. Makowitz and A. Ozkan for contributions to petrography, and to J. Gale, J. Holder, O. Ortega, R. Marrett, K. Milliken, and W. Narr for valuable discussions. The manuscript benefited from comments by Jim Evans, Julia Gale, Lana Dieterich, and an anonymous reviewer. Publication approved by the Director, Bureau of Economic Geology.

References

Anders, M.H., Wiltschko, D.V., 1994. Microfracturing, paleostress and the growth of faults. Journal of Structural Geology 16, 795–815.

Atkinson, B.K., 1984. Subcritical crack growth in geological materials. Journal of Geophysical Research 89, 4077–4114.

Bjørkum, P.A., Nadeau, P.H., 1998. Temperature controlled porosity/permeability reduction, fluid migration, and petroleum exploration in sedimentary basins. APEAJ, 453–464.

Dickinson, W.W., Milliken, K.L., 1995. The diagenetic role of brittle deformation in compaction and pressure solution, Etjo Sandstone, Namibia. Journal of Geology 103, 339–347.

Dietrich, D., Grant, P.R., 1985. Cathodoluminescence petrography of syntectonic fibers. Journal of Structural Geology 7, 541–553.

Dunne, W.M., Hancock, P.L., 1994. Paleostress analysis of small-scale brittle structures. In: Hancock, P.L., (Ed.), Continental Deformation, Pergamon Press, pp. 102–111.

Engelder, T., Fischer, M.P., 1996. Loading configurations and driving mechanisms for joints based on the Griffith energy-balance concept. Tectonophysics 256, 253–277.

Ferguson, H.G., Ganett, R.W., 1932. Gold quartz veins of the Alleghany district, California. U.S. Geological Survey No. 172, 139pp.

Fisher, D.M., Brantley, S.L., 1992. Models of quartz overgrowth and vein formation; deformation and episodic fluid flow in an ancient subduction zone. Journal of Geophysical Research 97 (13), 20043–20061.

Fowles, J., Burley, S., 1994. Textural and permeability characteristics of faulted, high porosity sandstones. Marine and Petroleum Geology 11, 608–623.

Gale, J.F.W., Laubach, S.E., Marrett, R.A., Olson, J.E., Holder, J.T., Reed, R.M., 2004. Predicting and characterizing fractures in dolomite reservoirs: using the link between diagenesis and fracturing, Geological Society of London Special Publication, Dolomite and Dolomitization, in press.

Hancock, P., 1985. Brittle microtectonics: principles and practice. Journal of Structural Geology 7, 437–457.

Hogg, A.J.C., Sellier, E., Jourdan, A.J., 1992. Cathodoluminescence of quartz cements in Brent Group sandstones, Alwyn South, UK North Sea. In: Morton, A.C., Haszeldine, R.S., Giles, M.R., Brown, S. (Eds.), Geology of the Brent Group. Geological Society Special Publication 61, pp. 421–440.

Holder, J., Olson, J.E., Philip, Z., 2001. Experimental determination of subcritical crack growth parameters in sedimentary rock. Geophysical Research Letters 28, 599–602.

Hulin, C.D., 1929. Structural control of ore deposition. Economic Geology 24, 15–49.

Johns, M.K., Laubach, S.E., Milliken, K.L., 1995. New microtextural evidence of syncementation fracturing in sandstone. Geological Society of America, Annual Meeting, Abstracts with Programs 27 (6), 216.

Labuz, J.F., Shah, S.P., Dowding, C.H., 1987. The fracture process zone in granite; evidence and effect. International Journal of Rock Mechanics and Mining Sciences & Geomechanics Abstracts 24, 235–246.

Lander, R.H., Walderhaug, O., 1999. Predicting porosity through

simulating sandstone compaction and quartz cementation. American Association of Petroleum Geologists Bulletin 83, 433–449.

Lander, R.H., Helset, H.M., Bonnell, L.M., Matthews, J.C., 1999. Implications of sandstone diagenesis for fluid overpressure development and seal failure. American Association of Petroleum Geologists Annual Convention, Abstracts 8, A76.

Lander, R.H., Gale, J.F.W., Laubach, S.E., Bonnell, L.M., 2002. Interaction between quartz cementation and fracturing in sandstone. American Association of Petroleum Geologists Annual Convention, Abstracts 11 (CD).

Laubach, S.E., 1988. Subsurface fractures and their relationship to stress history in East Texas Basin sandstone. Tectonophysics 156, 37–49.

Laubach, S.E., 1989a. Paleostress directions from the preferred orientation of closed microfractures (fluid-inclusion planes) in sandstone, East Texas Basin, U.S.A. Journal of Structural Geology 11, 603–611.

Laubach, S.E., 1989b. Fracture analysis of the Travis Peak Formation, western flank of the Sabine Arch, East Texas. The University of Texas at Austin, Bureau of Economic Geology Report of Investigations No. 185, 55pp.

Laubach, S.E., 1997. A method to detect fracture strike in sandstone. American Association of Petroleum Geologists Bulletin 81 (4), 604–623.

Laubach, S.E., 2003. Practical approaches to identifying sealed and open fractures. American Association of Petroleum Geologists Bulletin 87 (4), 561–579.

Marrett, R.A., Ortega, O.O., Kelsey, C., 1999. Power-law scaling for natural fractures in rock. Geology 27, 799–802.

Milliken, K.L., 1994a. The widespread occurrence of healed microfractures in siliciclastic rocks: evidence from scanned cathodoluminescence imaging. In: Nelson, P.A., Laubach, S.E. (Eds.), North American Rock Mechanics Symposium, Austin, Texas, Balkema, pp. 825–832.

Milliken, K.L., 1994b. Cathodoluminescence textures and the origin of quartz silt in Oligocene mudrocks, South Texas. Journal of Sedimentary Research A64, 567–571.

Milliken, K.L., 1996. Deformation bands formed by interrelated cementation and brittle fracture in porous sandstones, Hickory Formation, central Texas; synkinematic diagenesis revealed by cathodoluminescence imaging. American Association of Petroleum Geologists, Annual Convention, Abstracts 5, 98.

Milliken, K.L., Laubach, S.E., 2000. Brittle deformation in sandstone diagenesis as revealed by scanned cathodoluminescence imaging with application to characterization of fractured reservoirs. In: Pagel, M., Barbin, V., Blanc, P., Ohnenstetter, ?. (Eds.), Cathodoluminescence in Geosciences, Springer-Verlag, New York, pp. 225–243, Chapter 9.

Milliken, K.L., Reed, R.M., Laubach, S.E., 2004. Quantifying compaction and cementation within deformation bands in porous sandstones. American Association of Petroleum Geologists Memoir, Faults and Petroleum Traps, in press.

Misik, M., 1971. Observations concerning calcite veinlets in carbonate rocks. Journal of Sedimentary Petrology 41, 450–460.

National Research Council, 1996. Rock Fracture and Fluid Flow. National Academy Press.

Nelson, R.A., 1985. Geologic Analysis of Naturally Fractured Reservoirs. Gulf Publishing, Houston, 320pp.

Olson, J.E., 2004. Sublinear scaling of fracture aperture versus length: an exception or the rule? Journal of Geophysical Research, in press.

Olson, J.E., Pollard, D.D., 1989. Inferring paleostresses from natural fracture patterns: a new method. Geology 17, 345–348.

Olson, J.E., Holder, J., Qiu, Y., Rijken, M., 2001. Constraining the spatial distribution of fracture networks in naturally fractured reservoirs using fracture mechanics and core measurements. Society of Petroleum Engineers Paper, 71342.

Pagel, M., Barbin, V., Blanc, P., Ohnenstetter ?. (Eds.), 2000. Cathodoluminescence in Geosciences. Springer-Verlag, New York, 514pp.

Pollard, D.D., Aydin, A., 1988. Progress in understanding jointing over the past century. Geological Society of America Bulletin 100, 1181–1204.

Ramsay, J.G., 1980. The crack-seal mechanism of rock deformation. Nature (London) 284 (5752), 135–139.

Reed, R.M., Milliken, K.L., 2003. How to overcome imaging problems associated with carbonate minerals on SEM-based cathodoluminescence systems. Journal of Sedimentary Research 73 (2), 326–330.

Seyedolali, A., Krinsley, D.H., Boggs, S. Jr, O'Hara, P.F., Dypvik, H., Goles, G.G., 1997. Provenance interpretation of quartz by scanning electron microscope—cathodoluminescence fabric analysis. Geology 25, 787–790.

Walderhaug, O., Bjørkum, P.A., Nadeau, P.H., Langnes, O., 2001. Quantitative modeling of basin subsidence cause by temperature-driven silica dissolution and reprecipitation. Petroleum Geoscience 7, 107–114.

Wangen, M., 2001. A quantitative comparison of some mechanisms generating overpressure in sedimentary basins. Tectonophysics 334, 211–234.

Wiltschko, D.V., Morse, J.W., 2001. Crystallization pressure versus "crack seal" as the mechanism for banded veins. Geology 29, 79–82.